Safe Control for Structured Mobile Robotic Arm with Control Barrier Functions

Fan Ding[1], Han Wang[2], Jianping He[1], Yi Ren[3], and Yu Zheng[3]

Abstract— **Collision avoidance is a widely investigated topic in robotic applications. When applying collision avoidance techniques to a mobile robot, how to deal with the spatial structure of the robot remains a challenge. In this paper, we design a safe control law for the structured Mobile Robotic Arm (MRA) by solving a spatial structure-aware Quadratic Programming (QP), which is constrained by Control Barrier Functions (CBFs) based linear constraints. According to our proposed safe control algorithm, the safe control law is computed online and can successfully navigate the structured MRA to the desired state while avoiding collision with obstacles. The spatial structure of the MRA is incorporated in the QP by merging the rigid link restrictions into CBFs constraints. Simulations on a rigid rod and our modeled MRA are performed to verify the efficacy of the proposed method.**

I. Introduction

Mobile Robotic Arms (MRAs) are one kind of mobile robots consisting of robotic arms and mobile bases. With the spatial structures. MRAs allow more flexible operations to complete tasks of grasping and obstacle avoidance, and simultaneously introduces higher computational complexity. Regardless of the spatial structure, various techniques have been proposed in the past decades for collision avoidance problems, including Cell Decomposition [1], Potential Field Methods [2]) and heuristic methods (Fuzzy Logic Controller technique [3], Neural Network technique [4]). The readers are referred to [5] for an overview in this area. When applying these collision avoidance techniques to a structured mobile robot (i.e. MRA), the literature focuses on dealing with its spatial structure and high degrees of complexity (DOC).

As for dealing with the spatial structure of the mobile robot, existing approaches mainly use geometric envelopes to approximate and simplify the structure in the obstacle avoidance task. For instance, [6] enveloped the mobile robot and moving obstacles by spheres with different radii. And a mobile service robot, which is abstracted as a cylinder to navigate among movable obstacles was proposed in [7]. They addressed the obstacle avoidance problem by setting the minimum allowed distance with consideration to these radii. However, simplifying the structured mobile robots with geometric envelopes restricts its permitted workspace and its interaction with the environmental obstacles [7] (i.e. changing the structure in different surroundings).

[1]The Department of Automation, Shanghai Jiao Tong University, Shanghai, China. E-mails: {ding0106, jphe}@sjtu.edu.cn

[2]The Department of Engineering Science, University of Oxford, Oxford, United Kingdom. E-mail: {han.wang}@eng.ox.ac.uk

[3]The Tencent Robotics X Lab, Shenzhen, China. E-mails: {evanyren, petezheng}@tencent.com

The high degrees of complexity renders the calculation of control law for the MRA computationally expensive [8], if the spatial structure is fully considered. In [9], a hybrid teleoperation system was proposed to decouple the control of the mobile base and the manipulator, where the teleoperator carries out the motion control for the mobile base and the collision avoidance task is shifted to the manipulator subsystem. [10] proposed an optimization-based method to plan the obstacle avoidance motion for the MRA with the verification of the inverse kinematic calculation, which is not always guaranteed a feasible solution and requires much more calculation with the DOC increasing. Therefore, we expect to find an always feasible and computationally inexpensive method for the MRA to avoid collision with the obstacles.

Recently, the Control Barrier Functions (CBFs) approach is proposed as a promising and efficient tool for safe control [11]. By using a Quadratic Programming (QP) based framework, the safety requirements can be encoded as affine constraints. Significant success for this approach has been shown in robotics applications, especially in collision avoidance [12]. Extensions such as considering actuation capacity [13], safety-critical Lagrangian systems [14], MPC-CBF [15] for collision avoidance have been proposed. In the context of the safe control for multi-agent system in [13], the dimension of the multi-agent system is merged in the constraints of the CBFs-based QP. As the dimension of the agents increases, the amount of the constraints in the QP rather than the QP itself is to increase, which is proved to be time efficient [16].

In this paper, we aim at synthesizing a safe control law for a structured MRA. The proposed safe control law is able to drive the MRA to the desired state while avoiding collision with environmental obstacles. The challenge brought by the spatial structure is interpreted as the high degrees of complexity of the MRA. Inspired by [13], we propose to overcome the challenge by firstly introducing a CBFs based QP and then merging the high degrees of complexity into the constraints of the QP. The QP is solved in real time and with the DOC of the MRA increasing, the time consumption increases slightly. The main contributions are stated as follows:

- We synthesize a safe control law by solving a CBFs-based QP. This safe control law can successfully drive our modeled MRA to the desired state while avoiding collision with environmental obstacles.
- Our proposed approach incorporates the spatial structure of the MRA by merging the degrees of complexity into CBFs constraints and therefore the time consumption will not explode as the DOC increase.

The remainder of this paper is organized as follows. Preliminaries and reach-avoid task are specified in Section II. Safe control law for MRA with CBF is derived in Section III. Simulations are presented in Section IV. We conclude the paper in Section V.

II. Preliminaries and Problem Formulation

In this section, we first introduce the notion of safety, safety sets and present the forward invariant theorem based on the CBFs which renders the set of safe control laws. Then we give the problem formulation of safe control for MRA.

A. Control Barrier Functions

Throughout the paper, we consider a nonlinear control affine system:

$$\dot{x} = f(x) + g(x)u, \tag{1}$$

with $f(x)$ and $g(x)$ are locally Lipschitz, $x(t) \in D \subset \mathbb{R}^n$ and $u(x,t) \in U \subset \mathbb{R}^m$ represents the admissible input. Consider a set $\mathcal{C}$ defined as the zero super-level set of a continuously differentiable function $H(x) : D \to \mathbb{R}$ as:

$$\begin{aligned} \mathcal{C} &= \{x \in \mathbb{R}^n : H(x) \geq 0\}, \\ \partial\mathcal{C} &= \{x \in \mathbb{R}^n : H(x) = 0\}, \\ \mathrm{Int}(\mathcal{C}) &= \{x \in \mathbb{R}^n : H(x) > 0\}. \end{aligned} \tag{2}$$

Let $u = k(x)$ be a feedback controller such that the resulting dynamical system

$$\dot{x} = f_{cl}(x) = f(x) + g(x)k(x), \tag{3}$$

is locally Lipschitz. Due to the locally Lipschitz assumption, for any initial condition $x(0) \in D$, there exists a maximum interval of existence $I(x(0)) = [0, \tau_{max})$, such that $x(t)$ is the unique solution to (1) on $I(x(0))$; in the case when f_{cl} is forward complete [17], $\tau_{max} = \infty$. This allows us to define safety as follows.

Definition 1. A set $\mathcal{C}$ is forward invariant with respect to system (3) if for every initial state $x(t_0) \in \mathcal{C}$, there exists u, such that the solutions remain within $\mathcal{C}$, i.e., $x(t) \in \mathcal{C}$ for $\forall t \geq t_0$.

We refer to $\mathcal{C}$ as the safe set. If $\mathcal{C}$ is forward invariant, then the system (3) is safe. Before defining the formulation of control barrier functions, an extended class-$\mathcal{K}$ function, defined by $\alpha(\cdot) : (-b, a) \to (-\infty, \infty)$, is monotonicly increasing and $\alpha(0) = 0$. This allow us to define [18]:

Definition 2. Let $\mathcal{C} \subseteq D \subset \mathbb{R}^n$ be the super-level set of a continuously differentiable function $H(x) : D \to \mathbb{R}$. Then $H(x)$ is a control barrier function (CBF), if there exists an extended class-$\mathcal{K}$ function $\alpha(\cdot)$, such that $\forall x \in D$, for the control system (1) the following inequality holds:

$$\sup_{u \in U} \Big[\frac{\partial H(x)}{\partial x}(f(x) + g(x)u) \Big] \geq -\alpha(H(x)). \tag{4}$$

Remark 1. The conventional answer was to enforce $\dot{H}(x) \geq 0$ so that $\mathcal{C}$ is forward invariant. This may not be desirable since it requires all subsets of $\mathcal{C}$ to be invariant. A condition analogous to this was relaxed by [19] where the key idea was to only require a single subset to be invariant, thus resulting the condition (4). $\dot{H}(x) = \frac{dH(x)}{dt} = \frac{\partial H(x)}{\partial x}\frac{\partial x}{\partial t} = \frac{\partial H(x)}{\partial x}\dot{x}$.

Define $\mathrm{K}_{\mathrm{CBF}}(x)$ as the safe control law set:

$$\mathrm{K}_{\mathrm{CBF}}(x) = \Big\{ u \in \mathbb{R}^m : \frac{\partial H(x)}{\partial x}(f(x)+g(x)u) \geq -\alpha(H(x)) \Big\}. \tag{5}$$

Then, from Definition 2 we have that any $u(x) \in \mathrm{K}_{\mathrm{CBF}}(x)$ guarantees the set $\mathcal{C}$ forward invariant [17]. Suppose given a feedback control law $u = K(x)$ for the control system (1), it may be the case that $K(x) \notin \mathrm{K}_{\mathrm{CBF}}(x)$ for some $x \in D$. To modify this controller in a minimal way so as to guarantee safety, we consider the following Quadratic Program (QP) that finds the minimal perturbation on $K(x)$:

$$\begin{aligned} u(x) = \arg\min_{u \in U} \quad & \frac{1}{2}\|u - K(x)\|^2 \\ \text{s.t.} \quad & \frac{\partial H(x)}{\partial x}(f(x) + g(x)u) \geq -\alpha(H(x)). \end{aligned} \tag{CBF-QP}$$

B. Reach-Avoid Problem Formulation

Our goal is to design a feasible control law that drives a MRA to the desired state without collision with obstacles. Note that the degrees of complexity of the MRA come from the number of joints and rigid links. We model the MRA as follows:

- from the mobile base to the end-effector of the MRA, suppose there are N_{ep} joints, which are regarded by edge points labeled by a_i, $i = 1, \cdots, N_{\mathrm{ep}}$;
- refer the links between the edge points as line segments, denoted by A_i (A_i links a_i and a_{i+1}, link A_i can rotate around edge point a_i in a plane), $i = 1, \cdots, N_{\mathrm{ep}} - 1$. A_i could be regarded as a compact set in the space;
- describe the MRA $\mathcal{A}$ as a union of the links, where

$$\mathcal{A} = \bigcup_{i=1}^{N_{\mathrm{ep}}-1} A_i. \tag{6}$$

This allows us to call the MRA a multi-link system. To give problem formulation, we introduce edge point state $x^{(i)} \in \mathbb{R}^n$, rigid link state $x^{A_i} \subset \mathbb{R}^n$, and MRA state $X^{\mathcal{A}} \subset \mathbb{R}^n$. Note that these states are time-variant, so we rewrite them as $x^{(i)}(t)$, $x^{A_i}(t)$ and $X^{\mathcal{A}}(t)$.

Problem 1. Given a MRA workspace $\mathcal{X} \subset \mathbb{R}^n$, and divide it into an obstacle-occupied space $\mathcal{X}_{\mathrm{obs}} \subset \mathcal{X}$ and an obstacle-free space $\mathcal{X}_{\mathrm{free}} = \mathcal{X} \setminus \mathcal{X}_{\mathrm{obs}}$, find a feasible control law $u(x)$ that drives the MRA from the initial state (t_1) to the terminal state (t_2) while avoiding collision with the obstacles, i.e.

$$X^{\mathcal{A}}(t) \subset \mathcal{X}_{\mathrm{free}}, \quad t \in [t_1, t_2]. \tag{7}$$

III. Safe Controller Design for MRA with CBF

In this section, we synthesize the safe control law for the structured MRA with CBF-QP. The designed CBF-QP incorporates the spatial structure of the MRA by merging

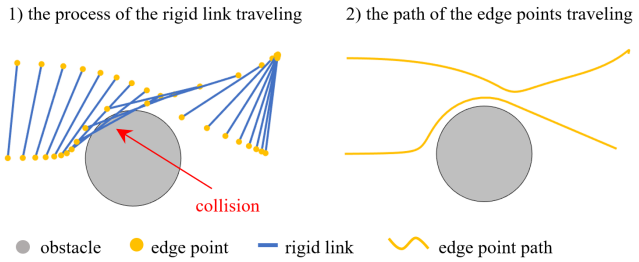

Fig. 1. The process of the rigid link and edge points movement. The rigid link forces fixed distance between any two connected edge points. By applying the CBF-QP method with rigid link restriction of distance, the rigid link collides with the obstacle but its edge points successfully avoid collision with the obstacle.

the rigid link restrictions into constraints. In this way, when the number of the edge points increases, we just need solve the same amount of the QP with increased constraints.

A. Obstacle-free Space Regeneration

To design the safe control for the MRA, we firstly start with exploring the safe control for its rigid links. Inspired by the multi-agent safe control in [13], we regard the two edge points of one rigid link as the two agents, and then respectively solve the (CBF-QP) for them. Moreover, we force a fixed distance between them. As illustrated in Fig. 1, the rigid link collides with the obstacle although the edge points successfully avoid collision with the obstacle in the navigation. In order to fill this gap, we propose to regenerate the obstacle-free space. The obstacle-free space is generally a non-convex set, as depicted in [20], which is the key point why the case in Fig. 1 happens. On the contrary, suppose the obstacle-free space $\mathcal{X}_{\text{free}}$ is a convex set, $\forall x^{(1)}, x^{(2)} \in \mathcal{X}_{\text{free}}$, equation:

$$\lambda \boldsymbol{x}^{(1)} + (1-\lambda)\boldsymbol{x}^{(2)} \in \mathcal{X}_{\text{free}}, \forall \lambda \in [0,1]$$

holds according to the convex set definition. This indicates that if the two edge points are within the convex set, then the rigid link connecting them is ensured in this convex set as well.

Therefore, we conduct the regeneration by extracting a series of convex sets (e.g. ellipsoids) $\mathcal{C}_k \subset \mathcal{X}_{\text{free}}$, $k = 1, \ldots, N$, from the original obstacle-free space [14]. From the start of the second convex set, each convex set has an intersection with the previous one. In order to satisfy the CBF conditions, we choose the ellipsoids as the convex sets for its convexity and compactness. Several algorithms can be used in order to find obstacle-free ellipsoids in the workspace and we refer [21] and [22] to the readers.

As for the transmission between the consecutive ellipsoids, given the initial state $X^{\mathcal{A}}_{(1)} \subset \mathcal{C}_1$ and the terminal state $X^{\mathcal{A}}_{(N+1)} \subset \mathcal{C}_N$ of the MRA, we assign the succeeded state $X^{\mathcal{A}}_{(k+1)}$ of the current expected state $X^{\mathcal{A}}_{(k)}$, $k = 1, \ldots, N-1$, by solving:

$$\begin{aligned} X^{\mathcal{A}}_{(k+1)} = \arg \max_{X^{\mathcal{A}}_{(k+1)} \subset \mathbb{R}^n} \quad & \frac{1}{2}\|X^{\mathcal{A}}_{(k+1)} - X^{\mathcal{A}}_{(k)}\|^2 \\ \text{s.t.} \quad & X^{\mathcal{A}}_{(k+1)} \subset \mathcal{C}_k \cap \mathcal{C}_{k+1}. \end{aligned} \tag{8}$$

Remark 2. Note that the ellipsoids $\mathcal{C}_k$ and $\mathcal{C}_{k+1}$ have a part of the overlapping area. The overlapping area can be tuned [22] so that it can accommodate the MRA, i.e., the constraint $X^{\mathcal{A}}_{(k+1)} \subset (\mathcal{C}_k \cap \mathcal{C}_{k+1})$ is solvable. The MRA system is ensured in these ellipsoids while transmitting between the consecutive ellipsoids.

B. State Space Model of the MRA System

Suppose we have a MRA (defined by (6)) with N_{ep} edge points and $N_{\text{ep}}-1$ links (with length l_i, $i = 1, \ldots, N_{\text{ep}}-1$):

State Space Model of the MRA System. The state of the edge points are regarded as their positions in the workspace ($x \in \mathcal{X} \subset \mathbb{R}^n$). 1) Assign the input of the system as:

$$u = [v^\top_{n_1 \times 1} \quad \dot{\theta}^\top_{(N_{\text{ep}}-1)\times 1}]^\top, \tag{9}$$

where $v_{n_1 \times 1} \in \mathbb{R}^{n_1}$ ($n_1 \leq n$) is the translation velocity vector, and $\dot{\theta}_{(N_{\text{ep}}-1)\times 1}$ is the rotation velocity vector. 2) For a_i, $i = 1, \ldots, N_{ep}$, choose the first one as the translation-velocity-driven edge point. The first edge point only possesses the translation velocity, so

$$\dot{x}^{(1)} = [v^\top_{n_1 \times 1} \quad \mathbf{0}^\top_{(N_{\text{ep}}-1)\times 1}]^\top. \tag{10}$$

3) For the rest of the edge points $x^{(i)}$, $i = 2, \ldots, N_{\text{ep}-1}$:

$$x^{(i)} = x^{(i-1)} + l_{i-1}\mathcal{F}(\theta^\top_{(i-1)\times 1}), \tag{11}$$

where $\mathcal{F}$ is a combination function of sine and cosine functions such that $\|\mathcal{F}(\theta_{(i-1)\times 1})\| = 1$. This indicates that $\|x^{(i)} - x^{(i-1)^\top}\| = l_{i-1}$, i.e., the distance between edge points a_{i-1} and a_i is fixed.

C. Safe Control for MRA with CBF

An ellipsoid can be described by the following equation:

$$(x - x_0)^\top B (x - x_0) = 1,$$

where B is a symmetric, positive definite matrix, $x \in \mathbb{R}^n$ and $x_0 \in \mathbb{R}^n$ representing the center of the ellipsoid. Recall that $\mathcal{C}$ in (2) is a super-level set of $H(x)$, and by applying $\mathcal{C}$ to encode obstacle-free ellipsoids as $\mathcal{C}_k$, $k = 1, \ldots, N$, we propose to define H directly from the generic equation of ellipsoids as H_k, $k = 1, \ldots, N$:

$$H_k(x) := 1 - (x - x_0)^\top B_i (x - x_0).$$

Edge Point CBF-QP. Safe control for one edge point (EP) can be achieved by (CBF-QP), specified as:

$$\begin{aligned} u(x^{(i)}) = \arg \min_{u \in \mathbb{R}^n} \quad & \frac{1}{2}\|u - K(x^{(i)})\|^2 \\ \text{s.t.} \quad & u \in \mathrm{K}^{(\mathrm{k})}_{\mathrm{CBF}}(x^{(i)}), \end{aligned} \tag{EP CBF-QP}$$

where,

$$\begin{aligned} \mathrm{K}^{(\mathrm{k})}_{\mathrm{CBF}}(x^{(i)}) = \Big\{ u \in \mathbb{R}^m : \Big[& \frac{\partial H_k(x)}{\partial x}(f(x) + g(x)u) \\ & + \alpha(H_k(x)) \Big] \Big|_{x = x^{(i)}} \geq 0 \Big\}. \end{aligned} \tag{12}$$

$x^{(i)}$ represents the state of the edge point a_i and $H_k(x)$ is the current ellipsoid. The $K(x^{(i)})$ is the previously computed

feedback controller that the (EP CBF-QP) is supposed to follow.

In the context of the extracted ellipsoids from the obstacle-free space, if the edge points are computed in one of the ellipsoids, then the rigid links connecting them are ensured in the ellipsoid, which indicates the union of these rigid links (i.e. MRA) is guaranteed in the ellipsoid. This allows us to extend (EP CBF-QP):

MRA CBF-QP. Safe control for MRA can be achieved by synthesizing the safe control for all the edge points:

$$u^* = \arg\min_{u\in\mathbb{R}^m} \quad \frac{1}{2}\|u - K(X^{\mathcal{A}})\|^2 \qquad \text{(MRA CBF-QP)}$$
$$\text{s.t.} \quad u \in \bigcap_{i=1}^{N_{\text{ep}}} \mathrm{K}_{\text{CBF}}^{(\text{k})}(x^{(i)}).$$

u^* is in the form of $u(X^{\mathcal{A}})$.

Remark 3. Note that $u \in \mathrm{K}_{\text{CBF}}^{(\text{k})}(x^{(i)})$ is a linear constraint. Given (10) and (11), $u \in \mathrm{K}_{\text{CBF}}^{(\text{k})}(x^{(1)})$ contains variables $v_{n_1\times 1}^\top$ and $u \in \mathrm{K}_{\text{CBF}}^{(\text{k})}(x^{(i)})$ contains variables $v_{n_1\times 1}^\top, \dot{\theta}_{i\times 1}^\top$, $i = 1, \ldots, N_{\text{ep}}$.

Proposition 1. The constraint of the (MRA CBF-QP), i.e., $u \in \bigcap_{i=1}^{N_{\text{ep}}} \mathrm{K}_{\text{CBF}}^{(\text{k})}(x^{(i)})$ is always solvable for the MRA system defined as (6) with state space model (10) and (11).

Proof. To prove with mathematical induction, we firstly consider the case when $N_{\text{ep}} = 1$. Then the constraint of the (MRA CBF-QP) becomes $u \in \mathrm{K}_{\text{CBF}}^{(\text{k})}(x^{(1)})$, which is always solvable.

Assume that when $N_{\text{ep}} = p \quad (p \geq 2)$, the constraint $u \in \bigcap_{i=1}^{N_{\text{ep}}} \mathrm{K}_{\text{CBF}}^{(\text{k})}(x^{(i)})$ is always solvable, then we need to prove when $N_{\text{ep}} = p + 1$, the conclusion still holds.

Let $N_{\text{ep}} = p + 1$, the constraint can be rewritten as:

$$u \in \bigcap_{i=1}^{p} \mathrm{K}_{\text{CBF}}^{(\text{k})}(x^{(i)}), \tag{13}$$

and at the same time,

$$u \in \mathrm{K}_{\text{CBF}}^{(\text{k})}(x^{(p+1)}). \tag{14}$$

Note that linear constraints (13) and (14) contain variables $v_{n_1\times 1}^\top$, $\dot{\theta}_{p\times 1}^\top$ and $v_{n_1\times 1}^\top$, $\dot{\theta}_{p\times 1}^\top$, $\dot{\theta}_{p+1}$ respectively. The (13) is always solvable, so we can find some $(v_{n_1\times 1}^\top, \dot{\theta}_{p\times 1}^\top)_\pi$ satisfying (13) and then substitute to (14) to find feasible $(\dot{\theta}_{p+1})_\pi$. Therefore, $(v_{n_1\times 1}^\top, \dot{\theta}_{p\times 1}^\top, \dot{\theta}_{p+1})_\pi$ is a feasible solution to $u \in \bigcap_{i=1}^{N_{\text{eq}}} \mathrm{K}_{\text{CBF}}^{(\text{k})}(x^{(i)})$ when $N_{\text{ep}} = p + 1$. □

A safe control algorithm for the MRA is proposed in Algorithm 1 (given threshold δ_1, δ_2 and maximum iteration I in one ellipsoid).

IV. Simulations

In this section, simulations of safe control for a rigid rod system and the MRA system are performed to verify the proposed algorithm. The QP solver is CVXGEN [23].

Algorithm 1: Safe Control Algorithm for MRA

Input: ellipsoids $\mathcal{C}_k$, $k = 1, \ldots, N$; MRA initial state $X_{(1)}^{\mathcal{A}} \subset \mathcal{C}_1$ and terminal state $X_{(N+1)}^{\mathcal{A}} \subset \mathcal{C}_N$.

```
for k = 1 : N do
    solve (8) for X^A_(k+1);
    acquire the present state of MRA X^A(t);
    if ||X^A(t) − X^A_(N+1)|| ≤ δ1 then
        break;
    end
    assign K(X^A) according to X^A_(k) and X^A_(k+1);
    for iter = 1 : I do
        if ||X^A(t) − X^A_(k+1)|| ≤ δ2 then
            break;
        end
        solve (MRA CBF-QP) for safe control law u*;
        update X^A(t) with u* and sample time Δt;
    end
end
```

A. Safe Control for Rigid Rod System in 2D Domain

We firstly consider a rigid rod system (with length l_1 and workspace $\mathcal{X} \subset \mathbb{R}^2$), which is actually a special case when $N_{\text{eq}} = 2$ for the MRA. According to (9), the input of the rigid rod system $u = [v_x, v_y, \dot{\theta}_1]^\top$, where v_x, v_y, $\dot{\theta}_1$ are the horizontal translation velocity, vertical translation velocity and the rotation velocity with which the second edge point rotates around the first edge point in the XY plane. According to (10), we assign the first edge point as:

$$\dot{x}^{(1)} = [v_x, v_y, 0]^\top,$$

and the second edge point as:

$$x^{(2)} = x^{(1)} + l_1[\sin\theta_1, \cos\theta_1]^\top.$$

As shown in Fig. 2(a), we aim at driving the rigid rod from the initial state to the end state without collision with the rectangle obstacles in a maze environment. According to the regeneration method, a series of 2D ellipses are extracted from the obstacle-free space shown in Fig. 2(b). The succeeded states in each pair of consecutive ellipses are calculated with (8) (drawn in Fig. 2(c)).

Then the safe control (illustrated in 3) is conducted for the rigid rod system following the Algorithm 1. In (MRA CBF-QP), we set the predefined controller as the pure proportional controller computed as a proportional gain times the distance between the present state of the system and its succeeded state. The extended class-$\mathcal{K}$ function is $\alpha(x) = x$.

B. Safe Control for MRA System in 3D Domain

We then consider the MRA system (workspace $\mathcal{X} \subset \mathbb{R}^3$) defined as (6). With the increasement of the value of N_{ep}, the structure of the MRA gets more complex (shown in Fig. 4) and the states of the edge points in the MRA system become more complicated.

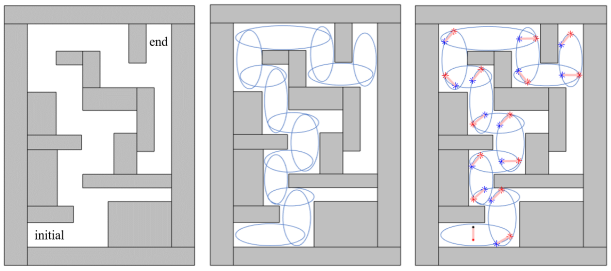

(a) maze environment (b) reprocess (c) succeeded states

Fig. 2. 2D maze environment and prep work of safe control. In the maze environment, grey rectangles are obstacles and obstacle-free space is obviously non-convex. By applying finding obstacle-free ellipses method [22] in the workspace, we reprocess the obstacle-free space and extract a series of consecutive-overlapped ellipsoids. Succeeded states in each pair of consecutive ellipses can be calculated once we set the initial θ_1. In Fig. 2(c), we regard the left bottom of the maze as the start and the right top as the end. We set $\theta_1 = \pi/2$ and the first edge point is painted red while the second one is painted blue.

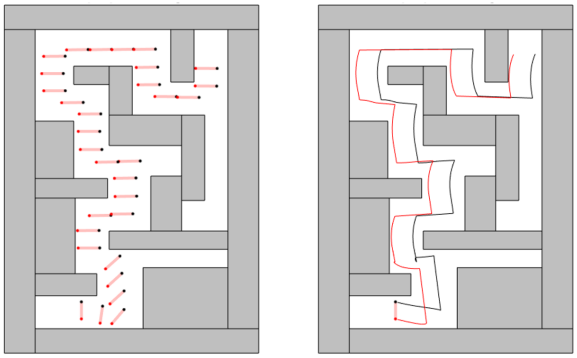

Fig. 3. The procedure of the safe control for rigid rod in maze environment. The left figure shows the states changing procedure and the right figure shows the path of the edge points. The rigid rod is driven from the initial state to the end state successfully without collision with the obstacles.

Example with $N_{\text{ep}} = 5$, we analyze the state space model of the MRA system. 1) Input

$$u = [v_x, v_y, \dot{\theta}_1, \dot{\theta}_2, \dot{\theta}_3, \dot{\theta}_4]^\top,$$

where v_x, v_y and $\dot{\theta}_i$ $(i = 1, 2, 3, 4)$ are the horizontal translation velocity, vertical translation velocity and the rotation velocity with which the $(i+1)$th edge point rotates around the (i)th edge point ($\dot{\theta}_1$ in XY plane, $\dot{\theta}_2$ in YZ plane, $\dot{\theta}_3$ in YZ plane, $\dot{\theta}_4$ in YZ plane). 2) The first edge point is assigned as:

$$\dot{x}^{(1)} = [v_x, v_y, \mathbf{0}_{4\times1}^\top]^\top.$$

3) Given length of the (i)th rigid link l_i , the states of the rest of the edge points (let $s_1 = \sin\theta_1$, $s_{23} = \sin(\theta_2 + \theta_3)$, $s_{234} = \sin(\theta_2+\theta_3+\theta_4)$, and $c_1 = \cos\theta_1$, $c_{23} = \cos(\theta_2+\theta_3)$, $c_{234} = \cos(\theta_2 + \theta_3 + \theta_4)$):

$$\begin{aligned}
x^{(2)} &= x^{(1)} + l_1 * [0, 0, 1]^\top, \\
x^{(3)} &= x^{(2)} + l_2 * [s_2c_1, s_2s_1, c_2]^\top, \\
x^{(4)} &= x^{(3)} + l_3 * [c_{23}c_1, c_{23}s_1, s_{23}]^\top, \\
x^{(5)} &= x^{(4)} + l_4 * [c_{234}c_1, c_{234}s_1, s_{234}]^\top.
\end{aligned}$$

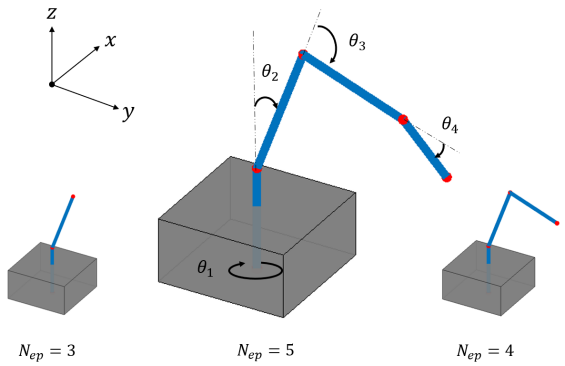

Fig. 4. The structure of the MRA with different values of N_{ep}. Here we enumerate the cases when $N_{\text{ep}} = 3$, $N_{\text{ep}} = 4$ and $N_{\text{ep}} = 5$. In the figure, edge points are painted red and the rigid links are painted blue. The grey base represents the mobile base and in the simulation, it is regarded as the first edge point which is hidden within it. The rotation rule of each edge points are also marked for the state space model analysis later of this subsection.

As shown in Fig. 6, we aim at driving the MRA from the initial state to the end state without collision with the obstacles in a 3D workspace. We reprocess the obstacle-free space of the workspace and a series of 3D ellipsoids are extracted from the obstacle-free space (Fig. 6(b)). The succeeded states in each pair of consecutive ellipsoids are calculated with (8) (6(c)).

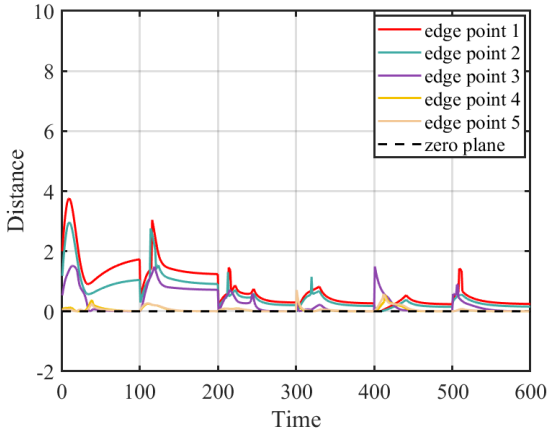

Fig. 5. The minimum distance of each edge point to the safe set boundary are depicted as curves of different colors. The edge point is in within the safe set if the distance is above zero plane, otherwise outside the present safe set.

Then we conduct the safe control for the MRA system following Algorithm 1. The predefined controller is set as the a proportional gain times the distance between the consecutive states of the MRA and the extended class-$\mathcal{K}$ function is $\alpha(x) = x$. The procedure of the safe control for the MRA system is illustrated in Fig. 7. The paths of the edge points are drawn in different color in Fig. 7(b) and for each edge point, we plot its minimum distance to the boundary of the present safe set, shown in Fig. 5. All the distances are above the zero plane and the curves tend to

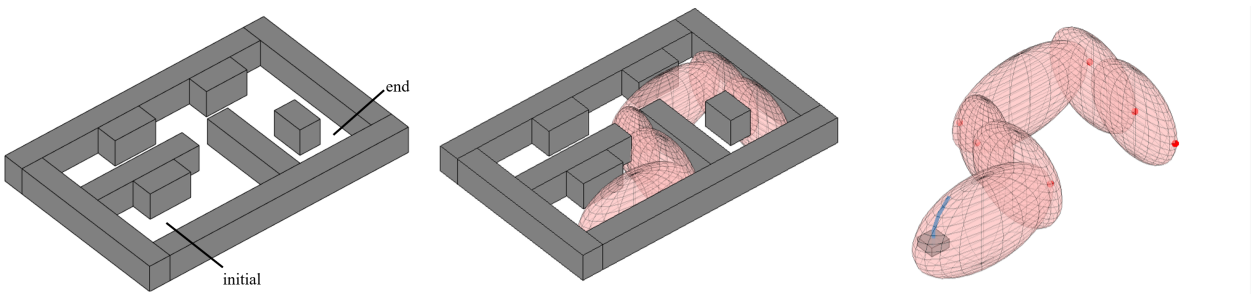

(a) 3D workspace (b) reprocess of the obstacle-free space (c) succeeded states

Fig. 6. 3D workspace and prep work of safe control. In the 3D workspace, the obstacle-free space is obviously non-convex and therefore we reprocess the obstacle-free space and extract a series of consecutive-overlapped ellipsoids [22], shown in Fig. 6(b). Succeeded states in each pair of consecutive ellipsoids can be calculated after specifying the initial state. In Fig. 6(c), we only mark the succeeded states of the first edge point (red points in pink ellipsoids) for a clearer look.

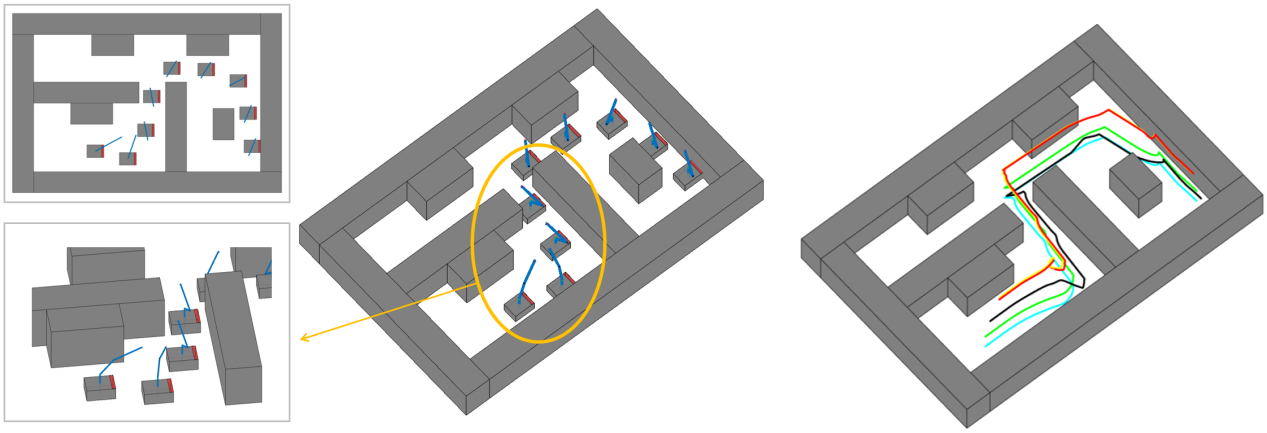

(a) procedure of the safe control (b) paths of the edge points

Fig. 7. Procedure of the safe control for the MRA. The MRA is set at an initial state, and if the MRA keeps the original structure, it will collide with the obstacles while passing the narrow road. Suppose the MRA is grasping some object so it has to stretch the links. With the safe control law solved by (MRA CBF-QP), we ensure the stretch of the links and guarantee the safety of the MRA. In the procedure of the navigation, the MRA changes its structure as a kind of interaction with the surroundings to avoid collision with the obstacles. The paths of the edge points are drawn in different colors shown in Fig. 7(b).

change approximately periodically with respect to time. This is reasonable because the MRA transmits though the series of the ellipsoids and in each ellipsoid follows the same steps of navigation.

Additionally, we test the time consumption of the (MRA CBF-QP) with different values of the N_{ep} (i.e. the degrees of the complexity of the MRA). Results of the time consumption for one iteration are listed as follows: 0.0230s ($N_{\text{ep}} = 2$), 0.0245s ($N_{\text{ep}} = 3$), 0.0259s ($N_{\text{ep}} = 4$), 0.0272s ($N_{\text{ep}} = 5$), 0.0282s ($N_{\text{ep}} = 6$), etc. As the value of N_{ep} increases, the time consumption increases slightly ($\leq 10\%$). The value of N_{ep} can be larger than "6" listed above and as long as the state space model of the MRA can be specified, the Algorithm 1 can work.

V. Conclusion and Future Direction

In this work we solve the problem of safe controller design for a structured MRA in an obstacle-clustered environment. To be exact, we design a spatial structure-aware QP, which is constrained by CBFs based linear constraints and propose the safe control algorithm for MRA. The safe control law is solved online and can successfully navigate the MRA to the desired state while avoiding collision with obstacles. Simulations of a rigid rod in 2D domain and the modeled MRA in 3D domain have been conducted to verify the feasibility of the algorithm. Additionally, the time consumption of our proposed method will not explode as the degrees of the complexity of the MRA increases. In the future we will apply our approach to physical test-bed and take the sensor-based obstacle-free space regeneration into consideration. To fill the gap between the simulations and the physical experiments, we will also consider to introduce the dilation process into the safe control for MRA.

References

[1] F. Lingelbach, "Path planning using probabilistic cell decomposition," in *IEEE International Conference on Robotics and Automation, 2004. Proceedings. ICRA'04. 2004*, vol. 1, pp. 467–472, IEEE, 2004.

[2] Y. Wang and G. S. Chirikjian, "A new potential field method for robot path planning," in *Proceedings 2000 ICRA. Millennium Conference. IEEE International Conference on Robotics and Automation. Symposia Proceedings (Cat. No. 00CH37065)*, vol. 2, pp. 977–982, IEEE, 2000.

[3] R. S. Sharma, S. Shukla, H. Karki, A. Shukla, L. Behera, and K. Venkatesh, "Dmp based trajectory tracking for a nonholonomic mobile robot with automatic goal adaptation and obstacle avoidance," in *2019 International Conference on Robotics and Automation (ICRA)*, pp. 8613–8619, IEEE, 2019.

[4] E. Rehder, F. Wirth, M. Lauer, and C. Stiller, "Pedestrian prediction by planning using deep neural networks," in *2018 IEEE International Conference on Robotics and Automation (ICRA)*, pp. 5903–5908, IEEE, 2018.

[5] A. Pandey, S. Pandey, and D. Parhi, "Mobile robot navigation and obstacle avoidance techniques: A review," *Int Rob Auto J*, vol. 2, no. 3, p. 00022, 2017.

[6] S. Qiu, H. Liu, Z. Zhang, Y. Zhu, and S.-C. Zhu, "Human-robot interaction in a shared augmented reality workspace," in *2020 IEEE/RSJ International Conference on Intelligent Robots and Systems (IROS)*, pp. 11413–11418, IEEE, 2020.

[7] M. Wang, R. Luo, A. Ö. Önol, and T. Padir, "Affordance-based mobile robot navigation among movable obstacles," in *2020 IEEE/RSJ International Conference on Intelligent Robots and Systems (IROS)*, pp. 2734–2740, IEEE, 2020.

[8] B. Sangiovanni, A. Rendiniello, G. P. Incremona, A. Ferrara, and M. Piastra, "Deep reinforcement learning for collision avoidance of robotic manipulators," in *2018 European Control Conference (ECC)*, pp. 2063–2068, IEEE, 2018.

[9] S. Thakar, P. Rajendran, H. Kim, A. M. Kabir, and S. K. Gupta, "Accelerating bi-directional sampling-based search for motion planning of non-holonomic mobile manipulators," in *2020 IEEE/RSJ International Conference on Intelligent Robots and Systems (IROS)*, pp. 6711–6717, IEEE, 2020.

[10] W. Li and R. Xiong, "Dynamical obstacle avoidance of task-constrained mobile manipulation using model predictive control," *IEEE Access*, vol. 7, pp. 88301–88311, 2019.

[11] A. D. Ames, J. W. Grizzle, and P. Tabuada, "Control barrier function based quadratic programs with application to adaptive cruise control," in *53rd IEEE Conference on Decision and Control*, pp. 6271–6278, IEEE, 2014.

[12] P. Glotfelter, J. Cortés, and M. Egerstedt, "Nonsmooth barrier functions with applications to multi-robot systems," *IEEE control systems letters*, vol. 1, no. 2, pp. 310–315, 2017.

[13] Y. Chen, A. Singletary, and A. D. Ames, "Guaranteed obstacle avoidance for multi-robot operations with limited actuation: a control barrier function approach," *IEEE Control Systems Letters*, vol. 5, no. 1, pp. 127–132, 2020.

[14] F. S. Barbosa, L. Lindemann, D. V. Dimarogonas, and J. Tumova, "Provably safe control of lagrangian systems in obstacle-scattered environments," in *2020 59th IEEE Conference on Decision and Control (CDC)*, pp. 2056–2061, IEEE, 2020.

[15] A. Thirugnanam, J. Zeng, and K. Sreenath, "Safety-Critical Control and Planning for Obstacle Avoidance between Polytopes with Control Barrier Functions," *arXiv e-prints*, p. arXiv:2109.12313, Sept. 2021.

[16] P. Bonami, O. Günlük, and J. Linderoth, "Globally solving nonconvex quadratic programming problems with box constraints via integer programming methods," *Mathematical Programming Computation*, vol. 10, no. 3, pp. 333–382, 2018.

[17] A. D. Ames, S. Coogan, M. Egerstedt, G. Notomista, K. Sreenath, and P. Tabuada, "Control barrier functions: Theory and applications," in *2019 18th European Control Conference (ECC)*, pp. 3420–3431, IEEE, 2019.

[18] A. D. Ames, X. Xu, J. W. Grizzle, and P. Tabuada, "Control barrier function based quadratic programs for safety critical systems," *IEEE Transactions on Automatic Control*, vol. 62, no. 8, pp. 3861–3876, 2016.

[19] L. Dai, T. Gan, B. Xia, and N. Zhan, "Barrier certificates revisited," *Journal of Symbolic Computation*, vol. 80, pp. 62–86, 2017.

[20] V. Vasilopoulos and D. E. Koditschek, "Reactive navigation in partially known non-convex environments," in *International Workshop on the Algorithmic Foundations of Robotics*, pp. 406–421, Springer, 2018.

[21] R. Deits and R. Tedrake, "Computing large convex regions of obstacle-free space through semidefinite programming," in *Algorithmic Foundations of Robotics XI*, pp. 109–124, Springer, 2015.

[22] A. Ray, A. Pierson, and D. Rus, "Free-space ellipsoid graphs for multi-agent target monitoring," *arXiv preprint arXiv:2205.15473*, 2022.

[23] P.-C. Aubin-Frankowski, N. Petit, and Z. Szabó, "Kernel regression for vehicle trajectory reconstruction under speed and inter-vehicular distance constraints," *IFAC-PapersOnLine*, vol. 53, no. 2, pp. 15084–15089, 2020.